

TRIPLE COVERS AND A NON-SIMPLY CONNECTED SURFACE SPANNING AN ELONGATED TETRAHEDRON AND BEATING THE CONE

GIOVANNI BELLETTINI, MAURIZIO PAOLINI, AND FRANCO PASQUARELLI

ABSTRACT. By using a suitable triple cover we show how to possibly model the construction of a minimal surface with positive genus spanning all six edges of a tetrahedron, working in the space of BV functions and interpreting the film as the boundary of a Caccioppoli set in the covering space. After a question raised by R. Hardt in the late 1980's, it seems common opinion that an area-minimizing surface of this sort does not exist for a regular tetrahedron, although a proof of this fact is still missing. In this paper we show that there exists a surface of positive genus spanning the boundary of an elongated tetrahedron and having area strictly less than the area of the conic surface.

1. INTRODUCTION

Finding a soap film that spans all six edges of a regular tetrahedron different from the cone of Figure 1 (left) is an intriguing problem. It was discussed by Lawlor and Morgan in [10, p. 57, and fig. 1.1.1], where a sketch of a possible soap film of positive genus is shown, based on an idea of R. Hardt¹; such a surface is here reproduced in Figure 1 (right)². The same picture was subsequently included in the book [12, fig. 11.3.2].

The cone constructed from the center of the solid spanning the six edges of the regular tetrahedron (Figure 1 left) has been proved to be area-minimizing³ if, roughly speaking, one imposes on the competitors the extra constraint that they divide the regular tetrahedron in four regions, one per face [15, Theorem IV.6], see also [10]. It corresponds to the actual shape that a real soap film attains when dipping a tetrahedral frame in soapy water; it includes a T -singularity at the center, where four triple lines (Y -singularities) converge from the four vertices satisfying the local constraints of an area-minimizing surface [15].

DIPARTIMENTO DI INGEGNERIA DELL'INFORMAZIONE E SCIENZE MATEMATICHE, UNIVERSITÀ DI SIENA, 53100 SIENA, ITALY, AND INTERNATIONAL CENTRE FOR THEORETICAL PHYSICS ICTP, MATHEMATICS SECTION, 34151 TRIESTE, ITALY

DIPARTIMENTO DI MATEMATICA E FISICA, UNIVERSITÀ CATTOLICA DEL SACRO CUORE, 25121 BRESCIA, ITALY

DIPARTIMENTO DI MATEMATICA E FISICA, UNIVERSITÀ CATTOLICA DEL SACRO CUORE, 25121 BRESCIA, ITALY

E-mail addresses: bellettini@diism.unisi.it, maurizio.paolini@unicatt.it, franco.pasquarelli@unicatt.it.

Date: March 1, 2022.

¹ A sketch of this surface was reportedly found by F. Morgan in R. Hardt's office during a visit at Stanford around 1988. F. Morgan and J. Taylor tried to find crude estimates to compare the two minimizers without success. Many years later R. Hardt himself told R. Huff about the problem, who then came out with the results that can be found in [9].

² The picture itself is a computer generated image obtained by J. Taylor using the **surface evolver** of K. Brakke.

³ That is, $(\mathbf{M}, 0, \delta)$ -minimal in the sense of F.J. Almgren [1].

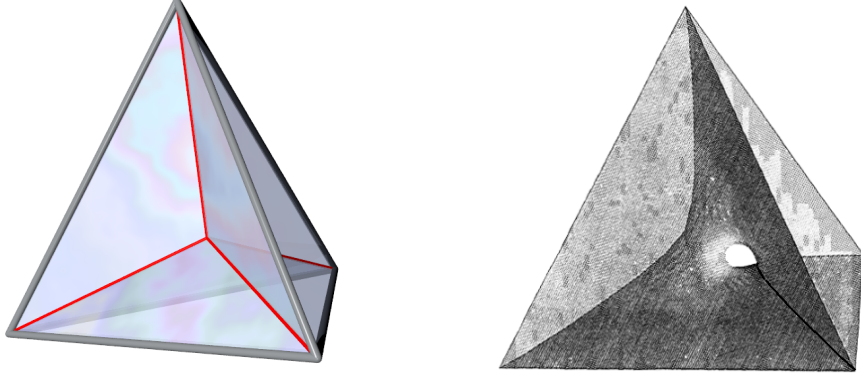


FIGURE 1. Left: the classic conical minimal film spanning a regular tetrahedron. Right: a slightly retouched version of [10, fig. 1.1.1]. In turn it is an enhanced version of [12, fig. 11.3.2]. Each triple curve “passes through” one of the two tunnels.

However, it is an open question whether a non-simply connected film, e.g. with “tunnels” connecting pairs of faces, could beat the cone; Figure 1 (right) shows a theoretically feasible configuration of such a minimizing film.

Although it seems a common opinion, based both on physical experiments and theoretical reasons, that such a surface does not actually exist (see e.g. [9]), to our best knowledge such a question still remains open.

Generalizations of the problem, for instance considering deformations of the tetrahedron with the addition of zig-zags [9], allows on the contrary to construct a surface with the required topology that at least satisfies all local properties of a minimal film. Another generalization that could lead to interesting minimizers consists in considering anisotropic surface energies [10].

The surface with positive genus⁴ depicted in Figure 1 includes two triple curves (curves where three sheets of the surface meet at 120°) and no quadruple points. Furthermore it sports two tunnels, one clearly visible that allows to traverse the tetrahedron entering from the front face and exiting from the back. The other hole is located on the other side of the film and allows to traverse the tetrahedron entering from the right lateral face and exiting from the bottom face (without crossing the soap film). Figure 10 in Section 6 helps to figure out the topological structure.

Our first result (Section 4, on the basis also of the computation of the fundamental group in Section 3) is the construction of a covering space of degree 3 of the complement of the one-skeleton of a tetrahedron, following the lines of [4] (see also [2]), that is compatible with Figure 1, right. Using covering spaces allows to treat in a neat way situations that seem hard to model using other approaches; see for instance Section 6.2, where we compare our approach with the Reifenberg approach.

A small portion of the soap film somehow behaves like a sort of “portal” to a parallel (liquid) universe. More precisely, each point in \mathbb{R}^3 , after removal of a suitable

⁴ This surface contains triple curves and boundaries, in this context we could not find a recognized definition of genus. However, if we remove the two flat portions, each bounded by a side of the tetrahedron and one of the two triple curves (operation that can be performed by deformation retraction, hence without changing the topological type), we end up with a surface without triple lines and bounded by a skew quadrilateral. We can then apply the formula $\chi = 2 - 2g - b$ where χ is the Euler characteristic ($\chi = -1$ in our case), g is the genus and $b = 1$ is the number of components of the boundary, obtaining $g = 1$. Consistently, the retracted surface can be deformed into a disk with a handle, or equivalently into a punctured torus.

set of curves (obtaining the so-called base space) has two other counterparts, for a total of three copies of the base space that are actually to be interpreted (locally) as three distinct sheets of a cover. Globally the picture is more interesting, since the covering space is constructed in such a way that when travelling along a closed curve in the base space, the “lifted” point might find itself on a different sheet of the same fiber. This can be used as a trick to overcome the problem in treating the soap film as transition between air and liquid. Since the liquid part has infinitesimal thickness, this would lead to the superposition of two layers, one corresponding to the air-liquid transition and the other to the transition back from liquid to air. For this reason an approach based e.g. on BV functions or Caccioppoli sets would lead to a liquid phase of measure zero and miss completely the two superposed layers. Using the covering space overcomes the problem by adding a “fake” big set of liquid phase, lying in a different sheet of the same fiber with an entry point corresponding to one face of the soap film and an exit point (reached travelling along suitable closed curves in the base space) from the other face in the same position. A phase parameter u defined in the covering space is then defined with values in $\{0, 1\}$, 0 indicating liquid, 1 indicating air, in such a way that in exactly one of the three points of a fiber we have $u = 1$ (air). Looping around an edge of the tetrahedron would take from one point to another of the same fiber, thus forcing the value of u to jump somewhere along the loop, which in turn would force the soap film to “wet” the edge.

The presence of triple curves implies that at least three sheets are required for a cover modelling the film problem, however the natural construction using suitable cyclic permutations of the three sheets when circling around each of the six edges of the tetrahedron cannot produce a surface with holes. This is because any path that traverses a tetrahedron entering from any face and exiting through another one is by topological reasons linked to exactly one of the edges and hence forced to traverse the film. Some way to distinguish tight loops around an edge and loops that encircle the edge far away is then required.

Hence the construction is more involved and requires the introduction of two “invisible wires”. This is done in the same manner and for similar reasons as in [4, Section 5.1], see in particular examples 7.7 and 7.8 in that paper. After constructing the covering space Y , we can adapt the machinery of [2] (see Section 5), and settle the Plateau problem in BV , with the differences that here the cut surfaces have selfintersections, and that the involved functions defined on Y , instead of taking values in an equilateral triangle (with barycenter at the origin) with the constraint of having zero sum on each fiber, take here values in $\{0, 1\}$, with the restriction indicated in (5.2) and discussed above.

Our next main result (Theorem 6.2) is to prove that, for a sufficiently elongated tetrahedron, there is a surface spanning its boundary, having the topology of the surface of Figure 1 right, and having area *strictly less* than the area of the conelike configuration. Therefore, if we allow for competitors of higher genus, we expect the conelike surface not to have minimal area. We remark that our result does not cover the case of a *regular* tetrahedron.

Positioning the invisible wires is delicate. Indeed, we would like the invisible wires not to influence the minimal film, which requires that the film does not wet them. This is not proved here, although the numerical simulations strongly support this fact for a sufficiently elongated tetrahedron and suitably positioned invisible wires. On the other hand, the discussion in Section 7 shows that a nonwetting relative BV -minimizer does not exclude the existence of an absolute minimizer with the structure of Figure 14, which we would like to exclude. Again, the numerical

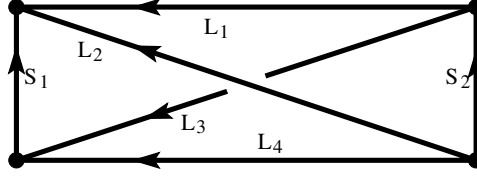


FIGURE 2. In view of the symmetry \mathbb{D}_{2d} of the desired surface, it is convenient to think of the tetrahedron as a wedge with two short edges, S_1 and S_2 , and four long edges, L_1, L_2, L_3, L_4 . When required, e.g. in (3.1), the short edges are oriented upwards, and the long edges are oriented from right to left.

simulations support the conjecture that if the invisible wires are positioned sufficiently far away from the short edges, then the absolute minimizer has the required topology and does not wet the invisible wires. On the contrary, positioning the invisible wires near the short edges would produce absolute minimizers that partially wet the invisible wires. We observe that soap films that partially wet a given curve were discussed in [1] and proved to exist for any knotted curve in [13]. In Section 8 we describe all possible triple covers of the base space among those producing soap films wetting all the edges of a tetrahedron. We conclude the paper with Section 9, where we describe the results of some numerical simulations, in particular varying the length of the long edges of a tetrahedron.

2. THE BASE SPACE

In view of the symmetry⁵ of the desired surface, it is convenient to think of the tetrahedron as a wedge with two short edges, S_1 and S_2 , and four long edges, L_i , $i = 1, \dots, 4$; for simplicity we name the one-skeleton of the wedge, i.e. the union of all edges, as $S = (\cup_{i=1}^2 S_i) \cup (\cup_{i=1}^4 L_i)$. A sketch of such a wedge is displayed in Figure 2.

In order to construct a proper base space for our cover let us summarize the required properties of the soap film that we would like to obtain.

- (1) The soap film is required to wet all six edges of the tetrahedron/wedge. From the point of view of a covering space this is achieved by requiring that any closed path that circles once around an edge at a short distance acts on the fiber with no fixed points;
- (2) it is possible to find closed paths that suitably traverse the tetrahedron (with reference to Figure 1, one path entering from the front face and exiting from the back face, the other entering from the right face and exiting from the bottom face) that when lifted to the covering space do not move at least one point of a fiber.

The second requirement seems at first sight incompatible with the first one, since such traversing paths are actually forced to circle once around a single edge of the tetrahedron. This is unavoidable and a consequence of the topology of the graph having the six edges as arcs. However these paths are allowed to circle the edges “far away”, and we can make the two paths, the one circling (say) the edge on the left (S_1 in Figure 2) at a short distance and the one traversing the visible hole in the soap film in Figure 1, not homotopically equivalent by introducing an obstruction in the base space in the form of an invisible wire, displayed as the left circle in Figure

⁵The symmetry group of the surface of Figure 1 (right) turns out to be \mathbb{D}_{2d} , using Schoenflies notation.

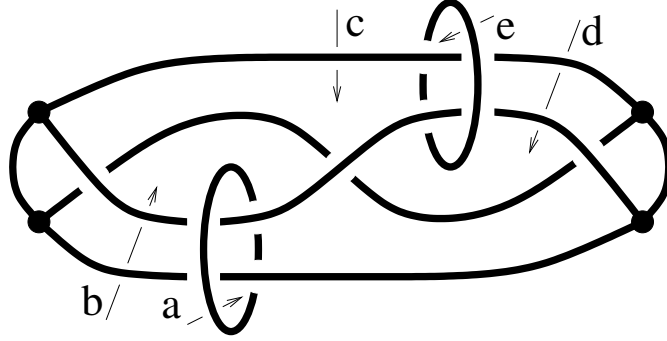


FIGURE 3. The base space M is \mathbb{R}^3 with the displayed arcs removed. Arrows and labels correspond to the generators of a presentation of the fundamental group.

3. The invisible wire has the purpose of making the two paths not equivalent, but in the meantime we do not want it to “perturb” the soap film.

We actually need to introduce two invisible wires, in the form of two closed loops C_1 , C_2 suitably interlaced to the edges of the wedge. We name their union as $C_{12} = C_1 \cup C_2$. The result is illustrated in Figure 3, the base space

$$M = \mathbb{R}^3 \setminus (S \cup C_{12})$$

being the complement in \mathbb{R}^3 of the system of curves displayed as thick lines. We shall use it to construct the covering space Y .

The picture follows the usual convention of inserting small gaps to denote *underpasses* of a curve below another. The four dots (vertices of the tetrahedron) represent points where three curves meet. This system of curves is the disjoint union of two loops (C_1 and C_2), a set of two short curves (S_1 , S_2) and four long curves (L_1 to L_4) joining four points. The latter is topologically equivalent to the set of edges of a tetrahedron.

Each of the two C_1 and C_2 loops around a pair of long edges, they are called *invisible wires* in [4] and their presence is essential to allow for jump sets (see Section 5) with the required topology. The loop C_1 is the one nearest to the short edge S_1 .

The quantity in the next definition plays an important role.

Definition 2.1. *Given a choice of the geometry of M , $\rho_\infty(M)$ is defined as the L^∞ -distance⁶ from the two short edges and the invisible wires of M :*

$$\rho_\infty(M) := \min\{\|x - \xi\|_\infty : x \in S_1 \cup S_2, \xi \in C_1 \cup C_2\} = \text{dist}_{L^\infty}(S_1 \cup S_2, C_1 \cup C_2).$$

Remark 2.2. In constructing the base space M we did not pay much emphasis on its geometry (see e.g. Figure 3), which is allowed as long as we study topological properties like its fundamental group, or when constructing the covering space Y .⁷ However, when considering the minimal film, the actual geometry becomes important. We shall then make specific choices both for the set of curves corresponding to the tetrahedral frame, straight segments with two different lengths, and for the two closed curves corresponding to the invisible wires. We point out here that the two invisible wires can be safely deformed into straight lines, one in the z direction through $(-s, 0, 0)$, the other in the y direction through $(s, 0, 0)$, for a suitable choice of $s > 0$, observing that a straight line is a closed curve in the compactification \mathbb{S}^3

⁶The L^∞ -norm $\|x\|_\infty := \max(|x_1|, |x_2|, |x_3|)$ is used here for convenience in view of the estimates to follow.

⁷It should be noted here that the base space M is path connected, locally path connected and semilocally simply-connected [7, Chapter 1.3].

of \mathbb{R}^3 . To avoid problems at infinity, where the two invisible wires would intersect, we can deform one or both of them “far away” (outside the convex hull of S).

Definition 2.3. *For two parameters $h > 0$ and $s \in (0, 1)$, we define a specific geometry for $M = M_{h,s}$ as follows. The four vertices of the wedge W are fixed at*

$$(h, \pm 1, 0), \quad (-h, 0, \pm 1), \quad (2.1)$$

and connected with straight segments of length $|S_1| = |S_2| = 2$, $|L_i| = \sqrt{2 + 4h^2}$, $i = 1, \dots, 4$. The invisible wires are now selected as straight lines $C_1 = \{(-sh, 0, t) : t \in \mathbb{R}\}$ and $C_2 = \{(sh, t, 0) : t \in \mathbb{R}\}$, (possibly modified far away from W).

The special value $h = \frac{\sqrt{2}}{2}$ results in a regular tetrahedron, whereas for $h > \frac{\sqrt{2}}{2}$ we have $|L_1| > |S_1|$.

Clearly, we have $\rho_\infty(M_{h,s}) = h(1 - s)$.

3. COMPUTING THE FUNDAMENTAL GROUP

We shall occasionally need to fix a base point m_0 in M . It is positioned far away from the set of curves, its actual position is inessential and we shall think of it as the eye of the observer. Equivalently, we can position it at infinity after compactification of \mathbb{R}^3 into \mathbb{S}^3 .⁸

The fundamental group $\pi_1(M)$ can be computed by using a technique similar to the construction of the Wirtinger presentation of a knot group. We position the base point m_0 above the picture and select a set of closed curves a, b, c, d, e that will serve as generators of the group. These curves (that represent elements of $\pi_1(M)$) are displayed in Figure 3 as arrows to be interpreted as curves that start at m_0 , run straight to the tail of one of the arrows, follow the arrow *below* one or two arcs of the system of curves and finally go back straight to m_0 .

In order to prove that a, b, c, d, e generate the whole fundamental group it is enough to construct curves that loop around each of the pieces of curves running from an underpass or node to another underpass or node.

As an example, the product $c^{-1}d$ is equivalent to a curve that loops around the piece of intermediate edge running from one disk to the other ($L_{2,2}$ in the notation fixed below). This can be seen by observing that loop d can be dragged from the right to the left of the top-right circle.

At this point we can construct $bc^{-1}d$ looping around the bottom-right piece of curve $L_{4,2}$ from the underpass to the lower-right node.

Curve $c^{-1}b$ corresponds to one of the four arcs ($L_{3,2}$ in the notation below) in which the long edge connecting the lower-left node to the upper-right one is divided. This can be seen by observing that modifying b by extending its head to pass under $L_{3,2}$ (Figure 3) gives a curve that is homotopic to c .

Traversing an underpass can be achieved by conjugation with the loop corresponding to the overpass, which allows to obtain all curves associated to the long edges. Product of two of these finally allows to loop around the short edges on the left and on the right. We end up with the following table, where the second index denotes what piece of the long arc of the wedge we are referring to (from left to

⁸Since a single point into a three-space cannot obstruct a closed path, adding the point at infinity to \mathbb{R}^3 does not impact the computation of the fundamental group, nor it will make any difference in the construction of the covering space. For that matter, it also makes no difference to substitute \mathbb{R}^3 with a big ball compactly containing the tetrahedron.

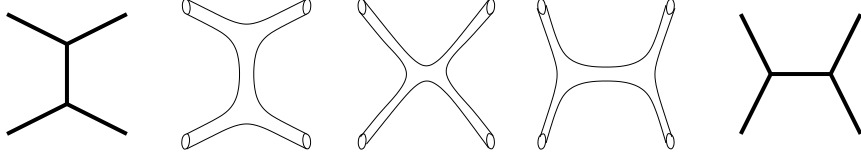


FIGURE 4. A tubular neighborhood of the Steiner tree on the left can be ambiently deformed into a tubular neighborhood of the Steiner tree on the right.

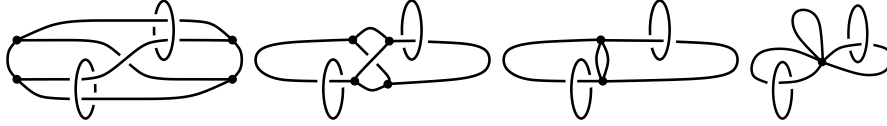


FIGURE 5. A sequence of steps showing that a tubular neighborhood of the system of curves can be ambiently deformed into a (tubular neighborhood of a) bouquet of three loops with two linked rings.

right):

$$\begin{aligned}
 L_{1,1} &\rightarrow c, & L_{1,2} &\rightarrow ece^{-1}, \\
 L_{2,1} &\rightarrow ac^{-1}da^{-1}, & L_{2,2} &\rightarrow c^{-1}d, & L_{2,3} &\rightarrow ec^{-1}de^{-1}, \\
 L_{3,2} &\rightarrow c^{-1}b, & L_{3,3} &\rightarrow d^{-1}bc^{-1}d, \\
 L_{4,1} &\rightarrow ad^{-1}cb^{-1}a^{-1}, & L_{4,2} &\rightarrow d^{-1}cb^{-1}, \\
 S_1 &\rightarrow ad^{-1}ca^{-1}c^{-1}, & S_2 &\rightarrow bc^{-1}ece^{-1}.
 \end{aligned} \tag{3.1}$$

We omit the values associated to $L_{3,1}$ and $L_{3,4}$ (readily deducible by conjugation due to traversal of, respectively, $L_{2,1}$ and $L_{2,3}$), since we shall not need them.

Each crossing provides a relation among the three curves involved. By collecting all such relations and simplifying we finally end up with the presentation (five generators and two relators)⁹

$$\pi_1(M) = \langle a, b, c, d, e; ab = ba, de = ed \rangle. \tag{3.2}$$

A different and more direct way to obtain the presentation (3.2) consists in an ambient deformation of a tubular neighborhood of the set of curves of Figure 3. An important remark here is that it is possible to flip the configuration of a “Steiner-like” pair of adjacent triple junctions as shown in Figure 4, without changing the homotopy type of both the set of curves and of its complement in \mathbb{R}^3 . This allows to transform the set of curves of Figure 3 by homotopy equivalence into the first configuration of Figure 5. Then we shrink two curves to a point in the passage from the second to the third configuration, and again one curve from the third to the last without modifications to the homotopy type of both the set of curves and of its complement in \mathbb{R}^3 .

Using this equivalence we can deform the set of curves as shown in Figure 5 to a bouquet of three loops with two linked rings, a configuration consistent with the presentation (3.2) for the fundamental group of the complement.

It should be noted that the graphs in the sequence of Figure 5 are not mutually homeomorphic, nor they are homeomorphic to the system of curves of Figure 3, whereas their complement in \mathbb{R}^3 is diffeomorphic. We have an ambient isotopy as soon as we substitute each system of curves with a small tubular neighbourhood.

⁹This is actually a right-angled Artin group.

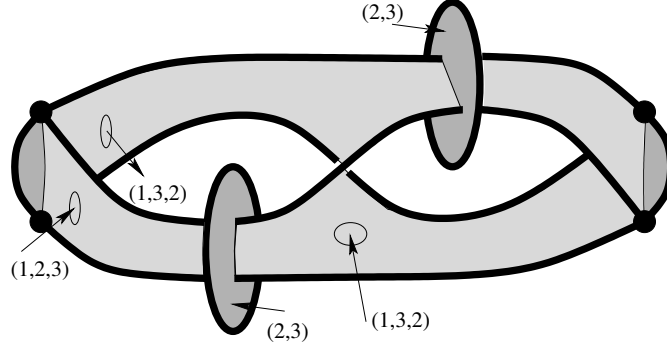


FIGURE 6. The cover is defined by a cut and paste technique on three copies of the base space cutted along the shaded surfaces. Local orientation is indicated, as well as the gluing among the sheets, with cycle notation.

4. THE TRIPLE COVER

The presence of triple curves in the soap film that we would like to reconstruct (Figure 1, right) implies that the covering space must be at least of degree three. There is no quadruple (tetrahedral) point in this film, so that three sheets for the cover might be sufficient.

However, the particular structure of the surface (a single smooth component of the film that arrives to a triple line from two distinct directions) requires special treatment, similar to that of Examples 7.7 and 7.8 of [4], with the introduction of the so-called *invisible wires*. These are introduced as two copies of \mathbb{S}^1 having the purpose of exchanging sheets 2 and 3, whereas sheet 1 is glued to itself.

As we shall see in Section 8 the introduction of the invisible wires is essential, in the sense that a cover with three (or two) sheets of the complement of the six tetrahedral edges is incompatible with the wetting conditions imposed on all edges.

A *cut and paste* construction of our cover is as follows [2].

- Take three copies of the base space M (complement in \mathbb{R}^3 of the system of curves shown in Figure 3): sheet 1, 2 and 3;
- cut them along the shaded surfaces¹⁰ displayed in Figure 6;
- glue the three sheets again in such a way that when crossing the large surface cut the three sheets are glued cyclically. When crossing the shaded disks sheets 2 and 3 get exchanged whereas sheet 1 on one side is glued to sheet 1 on the other side.

Remark 4.1 (Cutting locus as a stratified set). The set of cutting surfaces of Figure 6 (the cutting set) forms a stratification composed by seven pieces of (2D) smooth surfaces joined by four (1D) arcs (thin arcs in the picture, two triple curves and two selfintersection curves) and four (0D) end-points of the two selfintersection curves. The stratification as a whole is bounded by the set of curves defining M (thick curves in the picture) and by the four vertices of W . Each piece of 2D surface is orientable. The arrows indicate a choice of orientation, the two small lunette-like dark regions on the left and on the right are oriented from front to back (however

¹⁰The set of shaded surfaces and the system of curves give rise to a stratification, where the two-dimensional stratum (the cutting surfaces) is divided into connected components. The gluing permutation locally associated to each component can be transported along the whole component and must close consistently along closed paths on the surface. This would be a problem for non-orientable components (which is not our case) unless the permutation is of order two. In particular this is not an issue for covers of degree 2.

they are not a critic part of the cutting locus, see Remark 4.2) and finally the small portion of surface on the right of the upper disk is oriented from back to front, consistent with the orientation on the left of the disk. It should be noted that the large piece of surface connecting the two disks is subjected to a twist in the region near the center of the picture, so that the top portion is oriented from back to front. The gluing is based on the permutations shown in the picture (expressed in cycle notation) when crossing the surface in the direction of the arrows. Local triviality entails a constraint at the two intersection curves between the disks and the other surfaces: a tight loop around one of such intersections is contractible in M , hence the composition of the four permutations associated to crossings of the cuts (or their inverse if the loop crosses in the opposite direction with respect to the cut orientation) must give the identity. This results in a constraint upon the permutations on the left and on the right: they must be related by a conjugation defined by the transposition $(2, 3)$ associated to the disks. On the lunette surface to the left the permutation is $(1, 3, 2)$ when crossing from front to back. It cannot be chosen arbitrarily because of the local triviality property: a tight loop around the triple curve is contractible, hence the product of the three permutations associated to crossings of the cuts (or their inverse, according to orientation) must be the identity. Similarly, the permutation associated to the right lunette is forcibly given by $(1, 2, 3)$.

We denote by $p : Y \rightarrow M$ the cover defined in this way.

Remark 4.2. It is not actually necessary to use triple curves in the definition of the cover, indeed the left and right small fins could be removed and the two sides of the large surface could be extended up to the short lateral edges of the tetrahedral wedge. The chosen cut surface just mimics the structure that we expect for the minimizing film.

Remark 4.3. The local triviality of the cover allows to naturally locally endow the covering space Y with the euclidean metric induced by p from the euclidean structure of M .

Remark 4.4. The abstract construction in particular implies that, up to isomorphisms, the covering space constructed by cut and past is independent of the actual geometry of the cutting set, provided it has the same structure and the same gluing permutations at corresponding points. More precisely, the covering space is the same (up to isomorphisms) if the cutting set is deformed using a homeomorphism of \mathbb{R}^3 into itself with compact support and fixing the edges of W and the invisible wires C_{12} , and the gluing permutations are defined consistently.

4.1. The cover is not normal. The cover $p : Y \rightarrow M$ is clearly path connected. We claim that it is not normal [7, Chapter 1.3], as a consequence of the fact that sheet 1 is somehow specially treated by the gluing performed at the two disks. We recall that a cover is normal if for any pair $y, \eta \in Y$ with $p(y) = p(\eta)$ there exists a deck transformation¹¹ $\psi : Y \rightarrow Y$ with $\psi(y) = \eta$.

Proposition 4.5. *The cover $p : Y \rightarrow M$ is not normal.*

Proof. It is sufficient to show that the identity is the only deck transformation. Suppose by contradiction that ψ is a nontrivial deck transformation. Then ψ has no fixed points [7, page 70]. Now take $y \in p^{-1}(m_0)$ in sheet 1, m_0 being the base point of $\pi_1(M)$. Then $\psi(y)$ belongs to either sheet 2 or 3; suppose for definiteness that it belongs to sheet 2. If γ is a closed path in M corresponding to a (Fig. 3)

¹¹ A deck transformation is a homeomorphism $\psi : Y \rightarrow Y$ such that $p(\psi(\eta)) = p(\eta)$ for any $y \in Y$.

of $\pi_1(M)$, we can lift γ to Y into two distinct paths, one starting at y , the other starting at $\psi(y)$. These paths are mapped into each other by the homeomorphism ψ , however one is closed (the one starting at y), whereas the other is open, since when traversing the disk, the lifted path will continue on sheet 3. This gives a contradiction. \square

4.2. Abstract definition of the covering space. It is well known that an abstract definition of a covering space $p_{\text{abs}} : Y_{\text{abs}} \rightarrow M$ of M is based on selecting a subgroup H of $\pi_1(M)$, considering the set \widehat{Y} of paths $\gamma : [0, 1] \rightarrow M$ with $\gamma(0) = m_0$, and taking the quotient with respect to the equivalence relation

$$\gamma_1 \sim \gamma_2 \iff \gamma_1(1) = \gamma_2(1) \text{ and } [\gamma_1 \gamma_2^{-1}] \in H, \quad (4.1)$$

where γ_2^{-1} denotes the path γ_2 with opposite orientation, and defining the projection from \widehat{Y} to M as $[\gamma] \rightarrow \gamma(1)$. The degree of the cover is given by the index of H in $\pi_1(M)$. We shall describe a procedure to produce a subgroup H of index 3 in $\pi_1(M)$ (finitely presented in (3.2)) and subsequently prove in Theorem 4.7 that it gives a cover isomorphic to $p : Y \rightarrow M$.

In order to construct H we need a concrete way to identify its elements when written as words in the generators of the presentation (3.2). The first task is then to compute the actions $\sigma_a, \sigma_b, \sigma_c, \sigma_d, \sigma_e$ on the fiber $\{\hat{m}_0^1, \hat{m}_0^2, \hat{m}_0^3\}$ over the base point $m_0 \in M$ (the superscripts refer to the three sheets 1, 2, 3), corresponding to each generator in (3.2). This amounts in associating to each generator the resulting permutation induced on sheets 1, 2, 3. A quick check comparing Figures 3 and 6 suggests to define

$$\sigma_b = \sigma_d = (), \quad \sigma_a = \sigma_e = (2, 3), \quad \sigma_c = (1, 3, 2),$$

where $()$ denotes the identity permutation. Observe that σ_a and σ_b commute, as well as σ_d with σ_e , so that the two relators in (3.2) are consistent with these actions. Given an element of $\pi_1(M)$ expressed as a word w in the generators, by substituting these actions to the generators in w and performing the multiplications (left to right), we are then able to compute the action of the element represented by w on the fiber $\{\hat{m}_0^1, \hat{m}_0^2, \hat{m}_0^3\}$ in terms of a permutation of the three superscripts. H will then be recovered as consisting of those words that produce a permutation fixing $1 \in \{1, 2, 3\}$. Using relations satisfied by the actions σ_a through σ_e we can simulate the final multiplication after substitution in w by imposing such relations directly on the generators, the result would be the same. So we can safely add such relations to the presentation (3.2) as extra relators¹²

$$K := \langle a, b, c, d, e; ab = ba, de = ed, b, d, e = a, a^2, c^3, ca = ac^2 \rangle$$

to obtain a new group $K = \pi_1(M)/\hat{H}$ and a projection $q : \pi_1(M) \rightarrow K$, where \hat{H} is the normal subgroup of $\pi_1(M)$ generated by the added relators. A sequence of Tietze transformations [11] reduces the above presentation to $K = \langle a, c; a^2, c^3, ca = ac^2 \rangle$ which is quickly seen to be isomorphic to the symmetric group S_3 with representative elements $\mathcal{S} := \{a^\alpha c^\gamma : \alpha \in \{0, 1\}, \gamma \in \{0, 1, 2\}\} \subset \pi_1(M)$. Upon identification of the representative elements with their equivalence class, the projection q can be interpreted as a projection $q : \pi_1(M) \rightarrow \mathcal{S}$.

Finally, the subgroup $H \leq \pi_1(M)$ is defined as the set of $g \in \pi_1(M)$ such that $q(g) = 1$ if we write $q(g)$ as $q(g) = a^\alpha c^\gamma \in \mathcal{S}$. It corresponds to all paths in $\pi_1(M)$ that remain closed when lifted on Y with starting point \hat{m}_0^1 taken in sheet 1.

As an example, consider the word $w = ad^{-1}ca^{-1}c^{-1}$ (this word corresponds to looping once around the short edge S_1 , see (3.1)). We can remove all occurrences

¹²The presence of a^2, c^3 and $ca = ac^2$ in the list of relators is due to the fact that $\sigma_a^2 = \sigma_c^3 = ()$, and $\sigma_c \sigma_a = \sigma_a \sigma_c^2$.

of d (and of b , but there is none anyway, also we could substitute a for e if any occurrence of e were present) to obtain the word $aca^{-1}c^{-1}$. Enforcing $a^2 = c^3 = 1$ (empty word) we arrive at $acac^2$; using $ca = ac^2$ then produces a^2c^4 that finally reduces to the normal form $a^\alpha c^\gamma$, with $\alpha = 0$, $\gamma = 1$. Since $\gamma \neq 0$ we conclude that $w \notin H$.

Proposition 4.6. *The subgroup H has index 3 in $\pi_1(M)$ and it is not normal.*

Proof. That H is a subgroup is a direct check. Its right cosets are obtained by right multiplication by γ and γ^2 showing that there are exactly three cosets (they correspond to $\gamma = 0, 1, 2$ in \mathcal{S}). It is not a normal subgroup since $a \in H$ ($a = a^1c^0$, hence $\gamma = 0$), but $cac^{-1} \notin H$. Indeed $q(cac^{-1}) = q(ac)$ by enforcing $ca = ac^2$. The non normality of H is consistent with the non normality of the cover. \square

The next result ensures in particular that the approach of Section 5 is independent of the choice of the cut surface.

Theorem 4.7. *The cover $p_{\text{abs}} : Y_{\text{abs}} \rightarrow M$ defined by $H \leq \pi_1(M)$ is isomorphic to the cover $p : Y \rightarrow M$ defined with the cut and paste technique.*

Proof. The proof consists in a direct check that $\pi_1(M)$ defines the same action on the fiber over the base point $m_0 \in M$ [7, p. 70]. We first need to define a bijection between the two fibers $p^{-1}(m_0)$ and $p_{\text{abs}}^{-1}(m_0)$. In view of (4.1) the set $p_{\text{abs}}^{-1}(m_0)$ consists in equivalence classes of elements of $\pi_1(M)$ with respect to the equivalence relation $g_1 \sim g_2$ if and only if $g_1g_2^{-1} \in H$ (we slightly abuse the notation used in (4.1) for the equivalence relation and use it here on elements of $\pi_1(M)$ rather than on loops based on m_0). In other words $p_{\text{abs}}^{-1}(m_0)$ consists of the three right cosets of H in $\pi_1(M)$. This amounts in tagging the three right cosets with the numbers 1, 2, 3 and identifying the elements of $p^{-1}(m_0)$ and $p_{\text{abs}}^{-1}(m_0)$ with the same tag. Observe that Proposition 4.5 implies that there is a unique tagging that will induce the desired isomorphism. The three right cosets of H can be described as H , Hc and Hc^2 and will be tagged as 1, 3 and 2 respectively. It is now sufficient to check that the action of the generators a, b, c, d, e of $\pi_1(M)$ on the fibers gives the same permutation of the tagging (recall that in the abstract construction $\pi_1(M)$ acts on the fiber $p_{\text{abs}}^{-1}(m_0)$ as right multiplication). By comparing Figures 3 and 6 we see that c corresponds to the cyclic permutation (1, 3, 2) on $p^{-1}(m_0)$ and the same is true in the abstract construction in view of the chosen tagging. From the definition of H we see that $Ha = He = H$ whereas $Hca = Hce = Hc^2$, corresponding to the transposition (2, 3) of the tagged abstract fiber, the same as for the cut and paste construction. Finally, the two generators b and d clearly act as the identity on both $p^{-1}(m_0)$ and $p_{\text{abs}}^{-1}(m_0)$. \square

Remark 4.3 clearly applies to this construction of the covering space, so that the isomorphism of the covers constructed above is also an isometry.

4.3. Structure of the branch curves. The covering space Y , viewed as a metric space with the metric locally induced by the base space M , can be completed into \bar{Y} with the addition of *branch curves*. The projection p then naturally extends to

$$p : \bar{Y} \rightarrow \mathbb{R}^3$$

which will now be a branched cover.

Of particular importance are the branch curves corresponding to Cauchy sequences that converge in M to points belonging to the invisible loops C_1 and C_2 ; their structure allows to construct functions $u : Y \rightarrow \{0, 1\}$ whose $p(J_u)$ does not wet C_{12} , see Theorem 5.4.

As a direct consequence of the cut and paste construction of the cover, in particular of the fact that the permutation of sheets associated to the two disks fixes sheet 1 and swaps sheets 2 and 3, we have the following

Remark 4.8. The inverse image $p^{-1}(C_1)$ consists of two connected components, $p^{-1}(C_1) = C_1^1 \cup C_1^{23}$: C_1^1 being a curve containing no ramification points, i.e. having a small tubular neighborhood homeomorphic to its projection into a tubular neighborhood of $C_1 \subset \mathbb{R}^3$; C_1^{23} being a ramification curve of index two, i.e. having a small tubular neighborhood that projects onto its image as a branched cover of degree two. Similar properties hold for C_2 . Instead, the inverse image $p^{-1}(S)$ is connected with ramification index three.

5. THE MINIMIZATION PROBLEM

We refer to [3] for all details on functions of bounded variation; we denote by \mathcal{H}^ℓ the ℓ -dimensional Hausdorff measure in \mathbb{R}^3 , for $\ell = 1, 2$.

For any specific (geometric) definition of M (and hence of Y), we set

$$D_0^M(\mathcal{F}) := \left\{ u \in BV(Y; \{0, 1\}) : \sum_{y \in p^{-1}(x)} u(y) = 1 \text{ for a.e. } x \in M \right\}. \quad (5.1)$$

Then we impose a “Dirichlet” boundary condition at infinity, and the domain of the functional \mathcal{F} is defined as

$$D^M(\mathcal{F}) := \{ u \in D_0^M(\mathcal{F}) : u(y) = 1 \text{ for a.e. } y \in \text{sheet 1 of } p^{-1}(x), |x| > C \}, \quad (5.2)$$

for C large enough such that the ball of radius C compactly contains the solid wedge W . In view of the fact that the covering is not normal (Proposition 4.5), the choice of the Dirichlet condition is now quite important. If there is no risk of confusion we shall often drop the dependency on M and simply write $D_0(\mathcal{F})$ and $D(\mathcal{F})$ in place of $D_0^M(\mathcal{F})$ and $D^M(\mathcal{F})$.

Finally, the functional to be minimized is

$$\mathcal{F}(u) = \begin{cases} \frac{1}{2} |Du|(Y) & \text{if } u \in D(\mathcal{F}), \\ +\infty & \text{otherwise.} \end{cases}$$

The presence of the constant $1/2$ is due to the fact that, if u jumps at a point of a sheet, then the constraint in (5.1) forces u to jump also at the corresponding point (i.e., on the same fiber) of another sheet, while on the remaining sheet u does not jump. $|Du|$ is the usual total variation for the scalar-valued function u , and $|Du|(Y)$ can be defined using a partition of unity associated to a finite atlas of Y made of locally trivializing charts.

Given $u \in D_0(\mathcal{F})$, we denote by $J_u \subset Y$ the jump set of u .

Definition 5.1. A “film surface” is defined as $p(J_u) \subset M$, for $u \in D_0(\mathcal{F})$.

The film surface behaves well with respect to the jump set, in the sense that the total variation has the following representation, which specifies in which sense we are considering the notion of area:

Theorem 5.2. For all $u \in D_0(\mathcal{F})$ we have

$$\mathcal{F}(u) = \mathcal{H}^2(p(J_u)).$$

Proof. It is enough to repeat the arguments of [2, Lemma 2.12], by using local parametrizations of Y , and 2-rectifiability of the jump set of a BV -function. \square

Definition 5.3. For a given geometry of M , the minimum value of \mathcal{F} depends on M ; we set

$$\mathcal{F}_{\min}(M) := \inf_{u \in D_0^M(\mathcal{F})} \mathcal{F}(u)$$

and

$$\mathcal{S}_{\min}(M) := \{p(J_u) : u \in D_0^M(\mathcal{F}) \text{ and } \mathcal{F}(u) = \mathcal{F}_{\min}(M)\}.$$

By the semicontinuity and compactness properties of \mathcal{F} , the infimum on the right hand side is actually a minimum: this can be proven arguing as in [2]. We shall denote by $u_{\min} = u_{\min}(M)$ a function such that $\mathcal{F}(u_{\min}) = \mathcal{F}_{\min}(M)$ and by $\Sigma_{\min} = p(J_{u_{\min}}) = \Sigma_{\min}(M) \in \mathcal{S}_{\min}(M)$ the corresponding film surface (BV-minimizer). In particular the set of minimizing film surfaces $\mathcal{S}_{\min}(M)$ is nonempty.

Theorem 5.4 (Wetting condition). *Given $u \in D^M(\mathcal{F})$, the set $p(J_u)$ satisfies the following properties:*

- (P1) *any closed curve that loops around a long edge L_1, L_2, L_3 or L_4 intersects $p(J_u)$;*
- (P2) *any closed curve that loops around a short edge S_1 or S_2 at a distance smaller than $\rho_{\infty}(M)$ intersects $p(J_u)$.*

In particular, it is possible that a closed curve around S_1 or S_2 does not intersect $p(J_u)$.

By “loop around an edge” we mean that it can be continuously deformed without crossing any edge of the tetrahedron into a “meridian” of the edge, a loop that orbits around that edge alone at a small distance.

Proof. Let $x \notin p(J_u)$ and take the precise representative of u (still denoted by u , it satisfies the constraint in (5.1) in $M \setminus p(J_u)$). By construction of the covering space, a loop¹³ in M based at x around anyone of the long edges lifts into a path that moves all sheets of the fiber over x , in particular it moves the fiber where $u = 1$, taking it into a fiber where $u = 0$ (condition in (5.1)). This forces u to jump along the curve obtained by lifting the loop and gives (P1). Property (P2) is proved similarly by observing that a curve that loops around, say S_1 at a distance smaller than $\rho_{\infty}(M)$ cannot also interlace C_1 and again when lifted in the covering space it moves all points of the fiber. \square

The following definition is of central importance and highlights the essential feature of minimizers in order to be a “least area soap film” for an elongated tetrahedron.

Definition 5.5 (Non-wetting condition). *For a given geometry M we say that $\mathfrak{S} \in \mathcal{S}_{\min}(M)$ satisfies condition (NW) (non-wetting condition) if it does not intersect the invisible wires:*

$$\mathfrak{S} \cap C_{12} = \emptyset.$$

We say that the base space M satisfies condition (NW) if

$$\mathfrak{S} \cap C_{12} = \emptyset \quad \forall \mathfrak{S} \in \mathcal{S}_{\min}(M).$$

Remark 5.6. By compactness, if $\mathfrak{S} \in \mathcal{S}_{\min}(M)$ satisfies property (NW), there exists $\delta > 0$ such that Lipschitz deformations of \mathfrak{S} in $\mathbb{R}^3 \setminus S$ which are the identity out of a neighbourhood of \mathfrak{S} of size less than δ will not touch C_{12} , and can be recovered as jump set of some $u \in D(\mathcal{F})$. Hence \mathfrak{S} is $(\mathbf{M}, 0, \delta)$ -minimal in the sense of F.J. Almgren [1] and in particular satisfies the conditions proved by J. Taylor [15]

¹³ To get an element of $\pi_1(M)$ we need to select a path from m_0 to any point of the loop. The element of $\pi_1(M)$ consists in first moving along such path, then following the loop and finally going backwards to m_0 along the selected path. This does not impact the reasoning above.

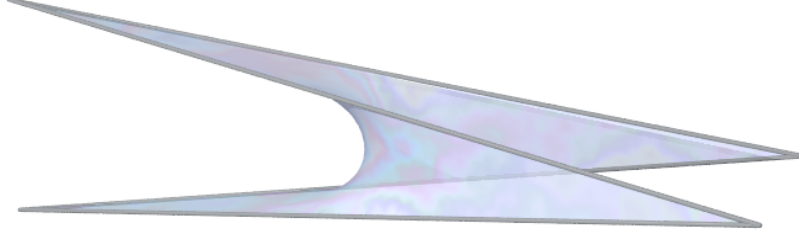


FIGURE 7. The minimal film spanning the long edges of W ($h = 3.5$).

of being locally either a minimal surface (zero mean curvature) or three minimal surfaces meeting along a curve at 120° . No T -singularity (quadruple point) can be present as a consequence of having only three sheets in the constructed covering. Moreover it is clear that \mathfrak{S} is not simply connected: any closed curve that loops around the front face of the tetrahedron along the edges, has nontrivial linking number with C_2 and therefore cannot be shrunk to a point by deformations on \mathfrak{S} .

5.1. Estimate of $\mathcal{F}_{\min}(M)$ from below. A crude estimate from below of $\mathcal{F}_{\min}(M)$ is a direct consequence of property (P1) above, indeed property (P1) is also satisfied by the minimal surface Σ_{skew} that spans the skew quadrilateral defined by the long edges L_i , $i = 1, 2, 3, 4$ (Figure 7). Hence

$$\mathcal{F}_{\min}(M) \geq \mathcal{H}^2(\Sigma_{\text{skew}}). \quad (5.3)$$

Remark 5.7. We have

$$2h \leq \mathcal{H}^2(\Sigma_{\text{skew}}) \leq \sqrt{4h^2 + 1} + 1. \quad (5.4)$$

The lower bound can be obtained by reasoning as in Theorem 5.8 below, whereas the upper bound is the area of the surface obtained by taking the upper and lower faces of W for $x < 0$, the central (unit) square $W \cap \{x = 0\}$ and the front and back faces for $x > 0$.

Set $M = M_{h,s}$ for a given choice of h and s . For any $u \in D(\mathcal{F})$, the projection $p(J_u)$ of the jump set of u satisfies properties (P1) and (P2) of Theorem 5.4. This allows us to obtain an estimate from below of its \mathcal{H}^2 measure, which refines estimates (5.3)-(5.4), see formula (5.7).

For $t \in [-1, 1]$ take the plane $\pi_t = \{x = ht\}$. Its intersection R_t with the wedge W is a rectangle of sides $1 + t$ and $1 - t$. We shall derive an estimate from below of $\mathcal{H}^1(p(J_u) \cap \pi_t)$.

5.1.1. Case $|t| > s$. Since $\rho_\infty(M) = h(1 - s)$, we have that the L^∞ -distance of π_t from S_2 if $t > 0$ (resp. S_1 if $t < 0$) is less than $\rho_\infty(M)$. As a consequence, any curve in the rectangle R_t that connects its two long sides can be closed as a loop around S_2 (resp. S_1) at an L^∞ -distance smaller than $\rho_\infty(M)$ and, in view of (P2) of Theorem 5.4, is forced to intersect $p(J_u) \cap \pi_t$. This, together with the first property, is enough to conclude¹⁴ that the length of $p(J_u) \cap \pi_t$ cannot be less

¹⁴ We have a “minimal partition” problem for the rectangle R_t into 3 sets, say A, B, C with the requirement that one long edge is contained in \overline{A} , the opposite long edge is contained in \overline{B} and both short edges are contained in \overline{C} . Since the local structure of a minimizer (boundary of an optimal partition) must satisfy the properties of a Steiner network, we only have a finite (and very small) set of possible configurations to consider.

than both the length of the Steiner tree joining the four vertices of R_t and twice the length of the long sides of R_t . Hence

$$\begin{aligned} \mathcal{H}^1(p(J_u) \cap \pi_t) &\geq \min\{1 + \sqrt{3} - (\sqrt{3} - 1)|t|, 2 + 2|t|\} \\ &= \begin{cases} 2 + 2|t| & \text{if } |t| < 2 - \sqrt{3}, \\ 1 + \sqrt{3} - (\sqrt{3} - 1)|t| & \text{if } |t| \geq 2 - \sqrt{3}. \end{cases} \end{aligned} \quad (5.5)$$

5.1.2. *Case $|t| \leq s$.* We can still enforce (P1) of Theorem 5.4: any curve in R_t connecting two adjacent sides can be completed into a loop around one of the long edges L_i , $i \in \{1, 2, 3, 4\}$ and hence it must intersect $p(J_u) \cap \pi_t$. It follows that the size of $p(J_u) \cap \pi_t$ cannot be less than twice the length of the short sides of R_t :

$$\mathcal{H}^1(p(J_u) \cap \pi_t) \geq 2 - 2t. \quad (5.6)$$

Theorem 5.8. *For a given choice of h and s , we have:*

$$\mathcal{F}_{\min}(M_{h,s}) \geq \begin{cases} 2h(4 - \sqrt{3} - 2s^2) & \text{if } s < 2 - \sqrt{3}, \\ h[3 + \sqrt{3} - 2(\sqrt{3} - 1)s - (3 - \sqrt{3})s^2] & \text{if } s \geq 2 - \sqrt{3}. \end{cases} \quad (5.7)$$

Proof. Let $u \in D(\mathcal{F})$.

Case $s < 2 - \sqrt{3}$. Using the tangential coarea formula [6, Theorem 3, pag. 103] and the sectional estimates (5.5) and (5.6), we have

$$\begin{aligned} \mathcal{H}^2(p(J_u)) &\geq \int_{-h}^h \mathcal{H}^1(p(J_u) \cap \pi_t) dt \\ &\geq 2h \int_0^s (2 - 2t) dt \\ &\quad + 2h \int_s^{2-\sqrt{3}} (2 + 2t) dt \\ &\quad + 2h \int_{2-\sqrt{3}}^1 [1 + \sqrt{3} - (\sqrt{3} - 1)t] dt \\ &= 2h[(2s - s^2) + (11 - 6\sqrt{3} - s^2 - 2s) + (5\sqrt{3} - 7)] \\ &= 2h(4 - \sqrt{3} - 2s^2). \end{aligned}$$

Case $s \geq 2 - \sqrt{3}$. The intermediate integral now disappears. We get

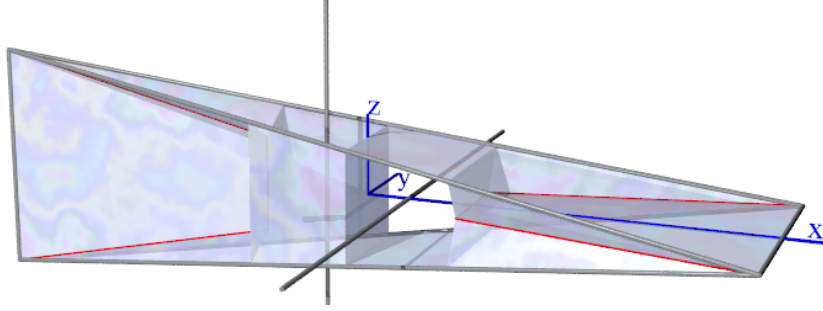
$$\begin{aligned} \mathcal{H}^2(p(J_u)) &\geq \int_{-h}^h \mathcal{H}^1(p(J_u) \cap \pi_t) dt \\ &\geq 2h \int_0^s (2 - 2t) dt \\ &\quad + 2h \int_s^1 [1 + \sqrt{3} - (\sqrt{3} - 1)t] dt \\ &= h[3 + \sqrt{3} - 2(\sqrt{3} - 1)s - (3 - \sqrt{3})s^2]. \end{aligned}$$

□

Note that for $s \rightarrow 0^+$ we obtain $\mathcal{H}^2(p(J_u)) \geq 2h(4 - \sqrt{3})$ and for $s \rightarrow 1^-$ we obtain $\mathcal{H}^2(p(J_u)) \geq 2h$ (compare with (5.4)).

6. A POSITIVE GENUS SURFACE BEATING THE CONELIKE CONFIGURATION

For a given $h > 0$ and $0 < s < 2 - \sqrt{3}$ we stick here with the choice of W (a solid elongated tetrahedron) given by Definition 2.3, i.e. with vertices having coordinates as in (2.1), see Figure 8, the regular tetrahedron corresponding to the choice $h = \frac{\sqrt{2}}{2}$.

FIGURE 8. Sketch of Σ with $\tau = 2 - \sqrt{3}$ and $h = 3.5$.

Let us denote by Σ_c a “conelike” film surface spanning the one-skeleton of W .

Definition 6.1 (Cone-like surface). *By “conelike set” (or “conelike film surface” if it has the appearance of a soap film) spanning the edges S of W we mean a set Σ_c that in W separates the four faces, i.e. such that it must intersect any path starting on one face, travelling in the interior of W and terminating on another face.*

The name “cone-like” is justified by the fact that we expect a minimal film with such separation property to be a deformed version of the minimizing cone of Figure 1 (left). In particular, a simply connected set in W containing S must separate the faces. Indeed, by contradiction if it does not separate the faces we can construct a closed path disjoint from the set that interlaces the path along the edges of a face. The set would then be non-simply connected (in particular non-contractible).

In Figures 1 left and Figure 11 we find two examples for a regular tetrahedron and an elongated tetrahedron.¹⁵ We shall compare Σ_c with a particular competitor Σ corresponding to (i.e., being the projection of) the jump set of a BV function u in the domain of the functional \mathcal{F} (Theorem 6.3); the competitor Σ will be non-simply connected.

We shall show that there exists $h > 1$ sufficiently large such that the area of Σ is less than the area of Σ_c (Theorem 6.2), giving quite strong evidence that Σ_c is not area-minimizing among minimal films if we allow for a more complex topology.

6.1. Constructing the surface Σ using the triple cover. Let $\tau \in (s, 1)$ be a parameter to be chosen later, see (6.8). The competitor Σ is constructed by joining five pieces,

$$\Sigma = \Sigma_1 \cup \Sigma_2 \cup \Sigma_3 \cup \Sigma_4 \cup \Sigma_v, \quad (6.1)$$

the first four obtained by sectioning the wedge with the three planes $\{x = 0\}$, $\{x = \pm h\tau\}$, see Figure 8, and the last one being “vertical”, as follows:

Case $x \in (-h, -h\tau)$ and $x \in (h\tau, h)$: the surface Σ_i , $i \in \{1, 4\}$ is chosen coincident with Σ_c , more precisely $\Sigma_1 := \Sigma_c \cap \{x < -h\tau\}$ and $\Sigma_4 := \Sigma_c \cap \{x > h\tau\}$.

Case $x \in (0, h\tau)$: the surface Σ_3 coincides with the top and bottom faces of W .

Case $x \in (-h\tau, 0)$: the surface Σ_2 coincides with the front and back faces of W .

In order to close the surface we need to add three “vertical” pieces, cumulatively denoted by Σ_v (see Figure 9), union of the square obtained by intersecting W with the vertical plane $\{x = 0\}$ and of the parts of the two rectangles resulting as the intersection of W with the two planes $\{x = \pm h\tau\}$.

¹⁵Note that for an elongated tetrahedron, an area-minimizing Σ_c does *not* satisfy the usual property of cones, of being invariant under multiplication $x \rightarrow rx$ for $r > 0$, see the caption of Figure 11. This is the reason for calling Σ_c a conelike configuration, and not simply a cone.

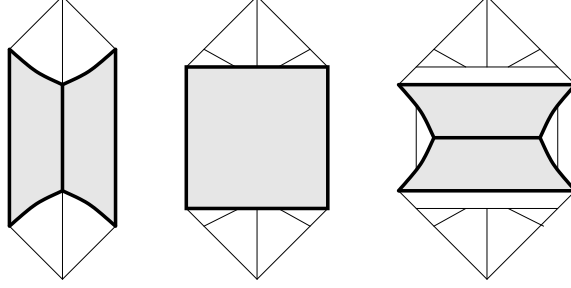


FIGURE 9. In grey the three components of Σ_v , vertical sections of Σ at $x = -h\tau$ (left), $x = 0$ (center), $x = h\tau$ (right). The area of these grey regions is estimated from above by their convex envelopes (see (6.6)).

Theorem 6.2. *Let $s \in (0, 2 - \sqrt{3})$. If $\tau \in (s, 1)$ is small enough and $h \in (1, +\infty)$ is large enough depending on τ , we have*

$$\mathcal{H}^2(\Sigma) < \mathcal{H}^2(\Sigma_c). \quad (6.2)$$

Proof. We have to show that

$$\mathcal{H}^2(\Sigma_1) + \mathcal{H}^2(\Sigma_2) + \mathcal{H}^2(\Sigma_3) + \mathcal{H}^2(\Sigma_4) + \mathcal{H}^2(\Sigma_v) < \mathcal{H}^2(\Sigma_c), \quad (6.3)$$

provided $\tau \in (s, 1)$ is small enough and $h = h(\tau) \in (1, +\infty)$ is large enough.

In view of the definition of Σ we have

$$\mathcal{H}^2(\Sigma_c \cap \{|x| > h\tau\}) = \mathcal{H}^2(\Sigma \cap \{|x| > h\tau\}),$$

and therefore inequality (6.3) is equivalent to

$$\mathcal{H}^2(\Sigma_2) + \mathcal{H}^2(\Sigma_3) + \mathcal{H}^2(\Sigma_v) < \mathcal{H}^2(\Sigma_c \cap \{-h\tau < x < h\tau\}). \quad (6.4)$$

As in Section 5, for $t \in [0, 1]$, the intersection of the plane $\pi_t = \{x = ht\}$ with the wedge W is a rectangle of sides $1 + t$ and $1 - t$. Since Σ_c divides W into four disjoint solid regions, one per face, it follows that $\Sigma_c \cap \pi_t$ divides the rectangle into four disjoint regions. Hence

$$\mathcal{H}^1(\Sigma_c \cap \pi_t) \geq 1 + \sqrt{3} - (\sqrt{3} - 1)t, \quad (6.5)$$

the right hand side being the length of the Steiner tree joining the four vertices of the rectangle.

For a given $\tau \in (s, 1)$ we shall need a bound from below of the section $\Sigma_c \cap \{-h\tau < x < h\tau\}$: using the coarea formula and (6.5), we have

$$\begin{aligned} \mathcal{H}^2(\Sigma_c \cap \{-h\tau < x < h\tau\}) &\geq \int_{-h}^h \mathcal{H}^1(\Sigma_c \cap \{-h\tau < x < h\tau\} \cap \pi_t) dt \\ &\geq 2h \int_0^\tau (1 + \sqrt{3} - (\sqrt{3} - 1)t) dt \\ &= 2(1 + \sqrt{3})h\tau - (\sqrt{3} - 1)h\tau^2. \end{aligned}$$

Therefore, in order to show (6.4) it is sufficient to prove

$$\mathcal{H}^2(\Sigma_2) + \mathcal{H}^2(\Sigma_3) + \mathcal{H}^2(\Sigma_v) < 2(1 + \sqrt{3})h\tau - (\sqrt{3} - 1)h\tau^2.$$

Since all intersection rectangles have the same perimeter and the central square has area equal to one, we have

$$\mathcal{H}^2(\Sigma_v) \leq 3, \quad (6.6)$$

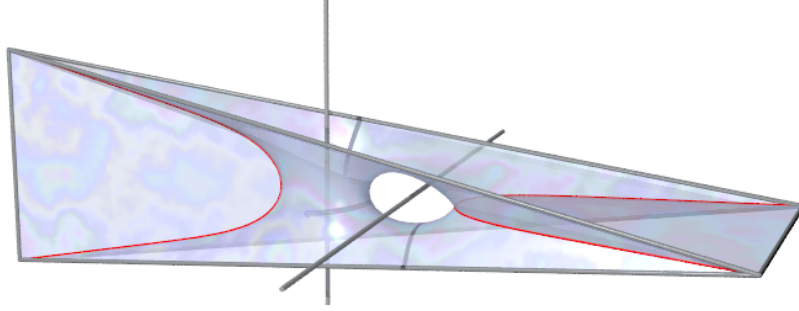


FIGURE 10. Minimal film obtained numerically starting a gradient flow from the Σ in (6.1), with $\tau = 2 - \sqrt{3}$ and $h = 3.5$. It satisfies property (NW) of Definition 5.5. Computation performed with the **surf** software code by Emanuele Paolini.

and so it will be sufficient to prove

$$\mathcal{H}^2(\Sigma_2) + \mathcal{H}^2(\Sigma_3) + 3 < 2(1 + \sqrt{3})h\tau - (\sqrt{3} - 1)h\tau^2. \quad (6.7)$$

Now, the area of the top (or bottom) facet F of W (the one having the vertex on the left and the basis on the right) equals $\sqrt{4h^2 + 1}$, therefore

$$\begin{aligned} \mathcal{H}^2(F \cap \{x < h\tau\}) &= \frac{(1 + \tau)^2}{4} \sqrt{4h^2 + 1}, \\ \mathcal{H}^2(F \cap \{0 < x < h\tau\}) &= \frac{(1 + \tau)^2}{4} \sqrt{4h^2 + 1} - \frac{1}{4} \sqrt{4h^2 + 1}. \end{aligned}$$

It follows

$$\mathcal{H}^2(\Sigma_2) + \mathcal{H}^2(\Sigma_3) = 4\mathcal{H}^2(F \cap \{0 < x < h\tau\}) = (2 + \tau)\tau\sqrt{4h^2 + 1},$$

so that (6.7) will be proved if we show

$$L := \frac{1}{h\tau} \left[(2 + \tau)\tau\sqrt{4h^2 + 1} + 3 \right] < 2(1 + \sqrt{3}) - (\sqrt{3} - 1)\tau =: R.$$

Let us select $\tau \in (s, 1)$ sufficiently small so that

$$4 + 2\tau < 2(1 + \sqrt{3}) - (\sqrt{3} - 1)\tau, \quad (6.8)$$

one possibility is e.g. to choose $\tau = 2 - \sqrt{3}$, consistent with $\tau \in (s, 1)$ in view of the constraint imposed on s . Then we have

$$\lim_{h \rightarrow +\infty} L = 4 + 2\tau < R,$$

and the result follows. \square

Inequality (6.8) is solved for $0 < \tau < 2(2 - \sqrt{3})$. Values leading to inequality (6.2) are e.g.

$$\tau = 2 - \sqrt{3}, \quad h = 16,$$

they lead to the values

$$\mathcal{H}^2(\Sigma) \approx 22.456 + c, \quad \mathcal{H}^2(\Sigma_c) \approx 22.585 + c$$

where c is the common value

$$c := \mathcal{H}^2(\Sigma_c \cap \{|x| > h\tau\}) = \mathcal{H}^2(\Sigma \cap \{|x| > h\tau\}),$$

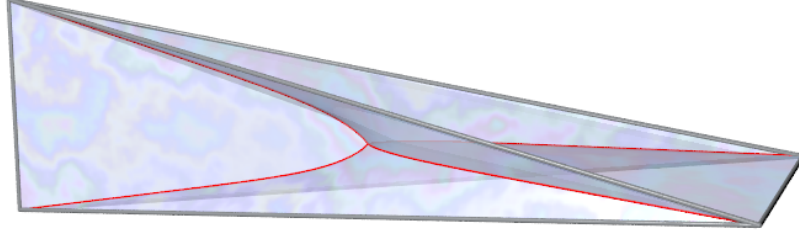


FIGURE 11. The conelike configuration Σ_c with $h = 3.5$. Note carefully that only the two crescent-like surfaces lying in $\{y = 0\}$ on the left and in $\{z = 0\}$ on the right are flat. Computation performed with the `surf` software code by Emanuele Paolini.

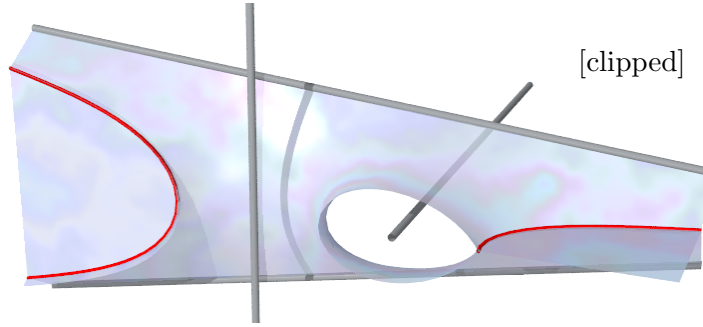


FIGURE 12. A zoom of the computed minimal surface of Figure 10 clipped at $y = -0.05$; the 120° condition can be clearly seen where the horizontal tunnel meets the triple line.

Theorem 6.3. *For any choice of $s \in (0, 2 - \sqrt{3})$ select the base space $M = M_{h,s}$ in Definition 2.3 with h large enough (e.g. $h > 16$). Let Σ be the competitor defined in (6.1). Then there exists $u \in D(\mathcal{F})$ such that $p(J_u) = \Sigma$. In particular, $\mathcal{F}(u) = \mathcal{H}^2(\Sigma)$, and*

$$\mathcal{F}_{\min}(M) < \mathcal{H}^2(\Sigma_c).$$

Proof. Fix $\tau = 2 - \sqrt{3}$ and let Σ be the corresponding competitor defined in (6.1). Since $s < 2 - \sqrt{3} = \tau$, it follows that the invisible wires do not intersect Σ and in view of Remark 4.4 we can assume that the cutting set in the cover construction is defined by Σ and then simply define $u : Y \rightarrow \{0, 1\}$ as 1 on the first sheet and zero otherwise. Clearly u satisfies the required constraints to ensure $u \in D(\mathcal{F})$ and in view of the gluing permutations (in particular u is locally constant, $u = 1$ on sheet 1 and $u = 0$ on sheets 2 and 3, on a neighborhood of $p^{-1}(C_{12})$, compare Figure 6) it is easy to show that $p(J_u) = \Sigma$, \square

Function u can also be constructed directly using the abstract definition of the covering (Section 4.2) as follows. First we need to fix an orientation and decide a permutation $\sigma \in S_3$ for each smooth portion of Σ . This is done consistently to the permutations of Figure 6, for example we associate the permutation $(1, 3, 2)$ to the left flat “lunette” when traversing it from front to back. We also need two “phantom” disks mimicking the cutting disks of figure 6 (with associated permutation $(2, 3)$) that cut e.g. the frontal trapezium with a vertical line in a right part

with permutation $(1, 3, 2)$ and a left part with permutation $(1, 2, 3)$ (when traversing it from front to back). The central vertical square would have the permutation $(1, 3, 2)$ associated to it when traversing from right to left. In a similar fashion we attach a suitable permutation to all the remaining (oriented) portions of the surface Σ , taking into account that the top trapezium is also divided in two parts by the phantom disk.

Now we first define a function \hat{u} on the set \hat{Y} of paths in M starting at the base point m_0 . If γ is such a path with $x := \gamma(1) \notin \Sigma$, we can suppose, up to a small deformation in the same homotopy class, that it has only transversal intersections with Σ and no intersections with the triple curves nor with the intersection of the phantom disks with Σ . Then we can enumerate the permutations associated to the intersections of $\gamma([0, 1])$ with Σ and the phantom disks or their inverse (based on whether γ traverses the surface in a positive or negative direction with respect to its selected orientation) and multiply all these permutations to obtain $\sigma_\gamma \in S_3$. If the final permutation fixes 1, i.e. $\sigma_\gamma(1) = 1$, then we define $\hat{u}(\gamma) = 1$, otherwise $\hat{u}(\gamma) = 0$.

The desired function $u : Y \rightarrow \{0, 1\}$ is now defined as $u([\gamma]) = \hat{u}(\gamma)$ where $[\gamma]$ is the equivalence class of γ in (4.1). It is necessary to show that this is a good definition, in other words, that $\hat{u}(\gamma_1) = \hat{u}(\gamma_2)$ whenever $\gamma_1 \sim \gamma_2$, i.e. whenever $[\gamma_1 \gamma_2^{-1}] \in H$. It is readily seen that this is a consequence of the stronger requirement that $\hat{u}(\gamma) = 1$ for all γ closed curve with $[\gamma] \in H$, which we now prove.

The choice of permutations on the pieces of surface is chosen such that the final permutation computed on a closed γ is insensitive to homotopic deformations of γ , so that we only need to show that σ_γ fixes 1 whenever $[\gamma] \in H$. This is true precisely because the choice of the permutations mimics the permutations used to define the covering by cut and paste displayed in Figure 6.

Remark 6.4. Inequality (6.2) is crucial in trying to actually prove the existence of a non-simply connected minimal film spanning an elongated tetrahedral frame, since it shows the existence of a surface with the desired topology having area strictly less than the minimal area achievable with conelike configurations. The candidate would be a minimizer of \mathcal{F} , since Theorem 6.3 implies that $\mathcal{F}_{\min}(M) < \mathcal{H}^2(\Sigma_c)$. However we still are unable to conclude, because we cannot exclude that the minimizing surface interferes with the invisible wires, i.e. it does not satisfy property (NW) of Definition 5.5 (see Section 7). Numerical simulations however strongly suggest that with appropriate choice of h and s in $M_{h,s}$ this is not the case (Figure 10).

6.2. Comparison with the Reifenberg approach. The approach of E. R. Reifenberg [14] to the Plateau problem is based on Čech homology. We want to show here that, presumably, the Reifenberg approach (in three space dimensions and in codimension one) cannot reproduce a surface with the topology as the one depicted in Figure 1, right.

One first fixes a compact¹⁶ abelian group G (for our purposes it is convenient to think of G as if $G = \mathbb{Z}$ even if this is not compact; in what follows the choice $G = \mathbb{Z}_m$ with various values for m leads to the same considerations). In the sequel all the homology groups are isomorphic to the direct sum $\bigoplus_{i=1}^r G$ of r copies of G , we shall refer to r as the *rank* of the homology group.

Next, given a compact subset S of \mathbb{R}^3 , one has to minimize the Hausdorff measure $\mathcal{H}^2(K)$ of K , among all compact sets $K \supseteq S$ in \mathbb{R}^3 satisfying a suitable condition, that we will specify. Here we fix S to be the union of the six edges of a tetrahedron.

¹⁶See [5] for an extension of the theory for a noncompact G .

The homology group $H_1(S; G)$ is seen to have rank 3, by observing that S is homotopic to a bouquet of three loops, and a convenient choice of the generators is:

- α : (counterclockwise) loop around the front face, described as $S_1^{-1}L_4^{-1}L_2$ with reference to Figure 2;
- β : loop around the top face, $L_2^{-1}S_2L_1$;
- ℓ : loop along the long edges, $L_4^{-1}L_2L_1^{-1}L_3$.

For some $K \supseteq S$ the inclusion $i : S \rightarrow K$ induces a homomorphism $i_* : H_1(S; G) \rightarrow H_1(K; G)$ between the first homology groups of S and K respectively, whose kernel is called algebraic boundary of K .

At this point for a given subgroup $L < H_1(S; G)$ we search for a minimizer of $\mathcal{H}^2(K)$ among all $K \in \mathcal{S}(L)$ where $\mathcal{S}(L)$ is the family of compact sets whose algebraic boundary contains L .

If V is a surface with the required topology (e.g. the one of Figure 10 or the one of Figure 8, or even that of Figure 1 right), we want on one hand $V \in \mathcal{S}(L)$ and on the other hand $\mathcal{S}(L)$ to be as small as possible, which leads to the choice $L = \ker(i_*)$.

The set V has first homology group $H_1(V, G)$ of rank two, generated by $i_*(\alpha)$ and $i_*(\beta)$, whereas ℓ is a generator of the kernel of i_* , leading to the choice of L as the subgroup of $H_1(S, G)$ generated by ℓ .

The family $\mathcal{S}(L)$ then contains subsets of \mathbb{R}^3 with first homology group of rank 2, containing S and with algebraic boundary L .

Unfortunately the imposed condition on the algebraic boundary does not impose wetting of the two short edges S_1 and S_2 , and indeed the surface of Figure 7 also is in $\mathcal{S}(L)$ and we presume it to be the Reifenberg minimizer.

7. POSITIONING THE INVISIBLE WIRES

For a fixed (sufficiently large) choice of h the minimum value $\mathcal{F}_{\min}(M) = \mathcal{F}(u_{\min})$ will depend on the relative position of the invisible wires C_{12} with respect to the tetrahedral frame. Our first guess would be that for a wide range of positions (those for which C_{12} does not touch $\Sigma_{\min} = p(J_{u_{\min}})$) such value is constant, and so is a minimizer of the functional.

When C_{12} leaves such a set of positions we would expect the minimum value to increase a bit, since in that case the invisible wires impose a further constraint on Σ_{\min} . Indeed the wires would “push” on the film surface and act as an obstacle for as long as the deformed surface bends at the wire with an angle larger than 120 degrees. This behaviour mimics the situation of a Steiner tree for three points vertices of an obtuse triangle with an angle larger than 120°.

Beyond the 120° threshold we expect one of the local “J. Taylor” rules [15] for a minimizing film to take effect and observe the formation of a new (fin-like) portion of the surface connecting a portion of C_{12} , let us call it the “wetted portion”, to a triple curve on the deformed surface meeting at angles of 120°.

The story is however completely different if C_{12} is moved to meet one or both of the two triple curves of the minimizing surface (red curves in Figure 10).

In this situation it is energetically favorable for the surface to suddenly jump into a configuration where a large portion of C_{12} is wetted by the flat part of the minimizer (Figure 13). Two new holes in the surface would then be created.

Actually this would be even more dramatic, since the formation of two smooth catenoid tunnels would come out in a situation where the tunnels are too long to be stable, so we also expect the tunnels to disappear completely with a final configuration resembling the one that would be obtained by a film that does not wet S_1 and S_2 with the addition of two flat trapezoid portions connecting e.g. S_1

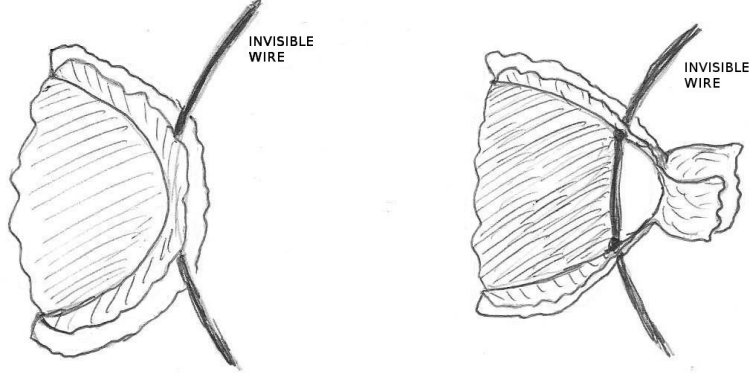


FIGURE 13. When the invisible wire approaches the triple curve (left) it becomes energetically convenient for the surface to jump into a configuration (right) where the invisible wire gets partially wetted (thus no longer invisible!) and a new hole is created right of the wire.

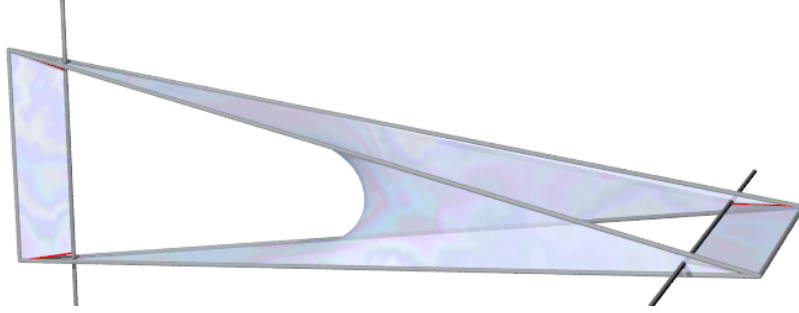


FIGURE 14. If the invisible wires approach the two short edges, the minimizer takes the structure shown in the picture ($h = 3.5$). The invisible wires are partially wetted by the film. Four short triple curves join the vertices of the frame with the boundaries of the wetted portion of the invisible wires. The structure of the film surface is different from that of Figure 10, in particular it does not satisfy property (NW) of Definition 5.5.

with part of C_1 and with the rest of the surface (similarly on the right), see Figure 14.

In order to rule out this possible minimizer we can derive a lower bound for the surface area in such a configuration.

Definition 7.1. For a given choice of $h > 0$ and $0 < s < 1$ and selecting $M = M_{h,s}$ we say that a film surface Γ is “Steiner-like” if it satisfies properties (P1), (P2) of Theorem 5.4¹⁷ and moreover the intersection $\Gamma \cap \pi_t$ with $\pi_t = \{x = ht\}$ and $|t| > s$ separates the four sides of the rectangle $W \cap \pi_t$.

Theorem 7.2. Let $s \in (0, 2 - \sqrt{3})$. A Steiner-like surface Σ_{steiner} can be modified into a surface Γ with the topology of the one constructed in Section 6.1 that does not wet the invisible wires and has lower area provided we choose $s \leq s_0$, s_0 small

¹⁷When $p(J_u)$ is replaced by Γ .

enough and then h large enough. Consequently Σ_{steiner} cannot be a minimizer of functional \mathcal{F} .

Proof. The proof mimics that of Theorem 6.2. We modify Σ_{steiner} in the region $-h\tau < x < h\tau$ with the choice $\tau = 2 - \sqrt{3}$ exactly as we did for Theorem 6.2 obtaining a surface Γ . Using again the coarea formula, the sectional estimate (5.5) with the second case also if $|t| < 2 - \sqrt{3}$ and (5.6), we have

$$\begin{aligned} & \mathcal{H}^2(\Sigma_{\text{steiner}} \cap \{-h\tau < x < h\tau\}) \\ & \geq \int_{-h\tau}^{h\tau} \mathcal{H}^1(\Sigma \cap \pi_t) dt \\ & \geq 2h \int_0^s (2 - 2t) dt + 2h \int_s^\tau [1 + \sqrt{3} - (\sqrt{3} - 1)t] dt \\ & = h[(2 + 2\sqrt{3})\tau - (\sqrt{3} - 1)\tau^2 - (2\sqrt{3} - 2)s - (3 - \sqrt{3})s^2], \end{aligned}$$

that has to be compared with

$$\mathcal{H}^2(\Gamma \cap \{-h\tau \leq x \leq h\tau\}) = (2 + \tau)\tau\sqrt{4h^2 + 1} + 3.$$

The only difference with the derivation of Theorem 6.2 is the presence of the two terms containing the parameter s . They however vanish as $s \rightarrow 0^+$, so that by selecting $s > 0$ sufficiently small we can again conclude if h is sufficiently large. \square

Specific values for s_0 and h turn out to be

$$s_0 = \frac{2 - \sqrt{3}}{4}, \quad h \geq 40$$

or

$$s_0 = \frac{2 - \sqrt{3}}{100}, \quad h \geq 16$$

The result of the previous theorem suggests the following

Conjecture 7.3. *Let $h > 16$ and $s = \frac{2 - \sqrt{3}}{100}$. Then $M_{h,s}$ satisfies condition (NW) of Definition 5.5.*

8. ALL POSSIBLE TRIPLE COVERS

We want to describe all possible covers of the base space M of degree 3 among those that will produce soap films that touch all six edges of the wedge and are not forced to touch the invisible circular wires. Here the fundamental group comes obviously into play, since we do that by describing all possible monodromy actions on the fiber above the base point m_0 . This monodromy action can equivalently be described as the action defined by a subgroup of $\pi_1(B)$ of index 3 by right multiplication.

Remark 8.1. The presence of triple points in the wireframe of the tetrahedron, together with the wetting condition (implying the existence of triple lines in the minimizing film) requires the presence of at least two distinct and nontrivial monodromy actions on the fiber at infinity, hence the cover has at least degree 3.

Remark 8.2. A degree 3 cover cannot allow for the standard (i.e., conelike) minimizing film for the tetrahedron. This is due to the presence of the central quadruple point of the minimizing film. Indeed we shall see that all covers satisfying the constraints will require a nontrivial monodromy action on the fiber when circling the invisible wires, making them an essential feature in the construction of the base space. Of course we could allow for more than two invisible wires.

Let H be a subgroup of $\pi_1(M)$ of index 3, and denote by $s_1 := H$, $s_2 := Hw_2$ and $s_3 := Hw_3$ its right cosets, for some choice of representative elements $w_2, w_3 \in \pi_1(M)$. The elements of $\pi_1(M)$ define an action on $\{s_1, s_2, s_3\}$ defined by $g : h \rightarrow hg$ (right multiplication by $g \in \pi_1(B)$). If h', h'' are in the same right coset then $h'g(h''g)^{-1} = h'(h'')^{-1}$ and the definition is wellposed.

We then have a map $\pi_1(M) \rightarrow S_3$ that to any element of $\pi_1(M)$ associates an element of the permutation group of the three cosets. A permutation of S_3 is interpreted as a permutation of the indices in $\{s_1, s_2, s_3\}$.

By composition, this map is defined once we know its value on the generators of $\pi_1(M)$.

In conclusion we have permutations $\sigma_a, \sigma_b, \sigma_c, \sigma_d, \sigma_e \in S_3$ (permutations of $\{1, 2, 3\}$) associated to the generators a, b, c, d, e respectively.

We now impose a number of constraints.

Consistency with relators: In the group presentation (3.2) the two relators must be consistent with the choice of the permutations $\sigma_a, \dots, \sigma_e$. In other words σ_a must commute with σ_b and σ_d must commute with σ_e . Take for example σ_a and σ_b ; they commute if and only if one of the following mutually exclusive conditions holds:

- (1) σ_a or σ_b is the identity permutation $()$;
- (2) σ_a and σ_b are both cyclic of order 3, hence a power of $(1, 2, 3)$;
- (3) $\sigma_a = \sigma_b$ are the same transposition.

Invisible-wire conditions: The soap film that we wish to model must not wet the two circular loops associated to generators a and e in Figure 3. In particular, a closed path starting at the base point in M and looping around one of such loops must not necessarily traverse the surface. Consequently the generators a and b must not move sheet 1 of the covering. The corresponding condition reads then as

$$\sigma_a, \sigma_e \in \{(), (2, 3)\}; \quad (8.1)$$

Wetting conditions: We want to reconstruct a film that spans all six sides of the wedge. In other words, any tight loop around these edges should cross the surface. This condition is somewhat tricky to impose, particularly in situations where the cover is not normal, because we need to state it on elements of $\pi_1(M)$, which requires to connect the base point to the tight loop. We end up with a condition that depends on *how* we choose the connecting path. Changing the path amounts to performing a conjugation on the element of $\pi_1(M)$. A strong wetting condition could be that any element in $\pi_1(M)$ that loops once around the selected edge must move all sheets (the permutation is required to be a derangement). This condition is insensitive to conjugation. We shall however require a weaker version of the wetting condition by requiring that the element of $\pi_1(M)$ moves sheet 1 (the sheet where $u = 1$ at the base point m_0 , far from W). This condition however depends on how we connect the tight loop to the base point. It seems only natural to require the connecting path to lie outside the wedge, which is not the same as requiring the corresponding Wirtinger-type loop in the diagram of Figure 3 to move sheet 1. In particular this is not true for L_3 , the long edge that in Figure 3 runs in the back and does not cross the two disks, for which a linking path that does not enter the wedge is bc^{-1} . In the end the (weak) wetting conditions read as:

$$\begin{aligned} \sigma_c, \quad \sigma_c^{-1}\sigma_d, \quad \sigma_b\sigma_c^{-1}, \quad \sigma_b\sigma_c^{-1}\sigma_d, \\ \sigma_a\sigma_d^{-1}\sigma_c\sigma_a^{-1}\sigma_c^{-1}, \quad \sigma_b\sigma_c^{-1}\sigma_e\sigma_c\sigma_e^{-1} \notin \{(), (2, 3)\} \end{aligned} \quad (8.2)$$

The third relation comes from $\sigma(L_{4,2})^{-1}\sigma(L_{3,3})\sigma(L_{4,2})$, where $\sigma(L_{i,j})$ is the permutation associated to the various long edges in (3.1), after substitution and simplification. It corresponds to a path that, as mentioned above, starts at m_0 , runs in the back of L_4 from below, then around L_3 , then again in the back of L_4 and back to m_0 . The fourth relation is the inverse of $\sigma(L_{4,2})$.

We shall now search for all possible choices of $\sigma_a, \sigma_b, \sigma_c, \sigma_d, \sigma_e$ that are compatible with the three set of constraints (8.1), (8.2) and consistency with the relators of the presentation.

Remark 8.3. Our search also includes the special cases where one or both of the invisible wires C_1 and C_2 are not present, since the choice, say, $\sigma_a = ()$ leads to the same result as removal of C_1 .

We separately analyze the possibilities with all choices of σ_a and σ_e allowed by (8.1) arriving to the conclusion that the presence of both invisible wires is essential.

8.1. Searching covers for $\sigma_a = \sigma_e = ()$. First note that all constraints above are insensitive to exchange of sheets 2 and 3. This means that for definiteness we can assume that $\sigma_c(1) = 2$, which in view of the first wetting constraint in (8.2) leaves us with only two possibilities: $\sigma_c = (1, 2)$ or $\sigma_c = (1, 2, 3)$.

8.1.1. Case $\sigma_c = (1, 2, 3)$. Wetting constraints 2, 3, 5, 6 imply $\sigma_d \in \{(1, 3, 2), (1, 2)\}$ resulting in $\sigma_c^{-1}\sigma_d$ sending $3 \mapsto 1$. Moreover $\sigma_b \in \{(1, 3, 2), (1, 3)\}$ resulting in σ_b sending $1 \mapsto 3$. This would imply $\sigma_b\sigma_c^{-1}\sigma_d$ sending $1 \mapsto 1$, contrary to wetting constraint 4.

8.1.2. Case $\sigma_c = (1, 2)$. Wetting constraints 2, 3, 5, 6 imply $\sigma_d \in \{(1, 2, 3), (1, 3)\}$ resulting in $\sigma_c^{-1}\sigma_d$ sending $3 \mapsto 1$. Moreover $\sigma_b \in \{(1, 3, 2), (1, 3)\}$ resulting in σ_b sending $1 \mapsto 3$. This would imply $\sigma_b\sigma_c^{-1}\sigma_d$ sending $1 \mapsto 1$, contrary to wetting constraint 4.

8.2. Searching covers for $\sigma_a = ()$ and $\sigma_e = (2, 3)$. Again we can assume that $\sigma_c(1) = 2$.

Reasoning as before, from $\sigma_a = ()$ we get $\sigma_d \in \{(1, 3, 2), (1, 2, 3), (1, 2), (1, 3)\}$. However σ_d and σ_e must commute, which is incompatible with $\sigma_e = (2, 3)$.

8.3. Searching covers for $\sigma_a = (2, 3)$ and $\sigma_e = ()$. Again we can assume that $\sigma_c(1) = 2$.

Reasoning as before from $\sigma_e = ()$ we get $\sigma_b \in \{(1, 3, 2), (1, 2, 3), (1, 2), (1, 3)\}$, which does not commute with σ_a .

8.4. Searching covers for $\sigma_a = \sigma_e = (2, 3)$. Consistency with the relators of the group presentation leads to

$$\sigma_b, \sigma_d \in \{(), (2, 3)\}, \quad \sigma_c \notin \{(), (2, 3)\}.$$

A direct check shows that any choice satisfying the requirements above also satisfies all constraints for our covering.

Figure 15 shows the cover that corresponds to the choice

$$\sigma_b = \sigma_d = (), \quad \sigma_c = (1, 2).$$

The resulting cover is clearly not isomorphic to the one constructed in Section 4 and it is a natural question whether the minimization problem $\mathcal{F}(u) \rightarrow \min$ in this context leads to the same result. This is entirely possible but we do not want to pursue the subject here.

On the other hand we actually can find functions $u \in D(\mathcal{F})$ (with $D(\mathcal{F})$ redefined based on the new covering) with a jump set that is incompatible with the former

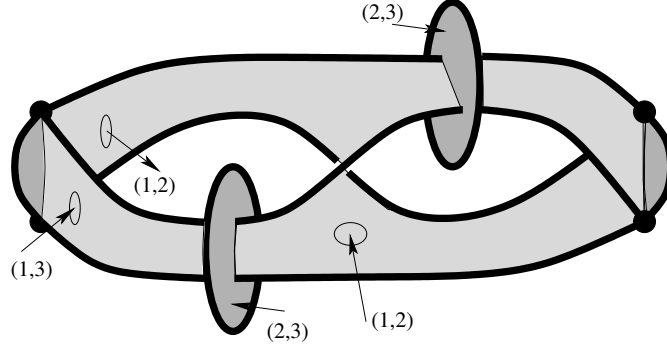


FIGURE 15. An alternative covering definition that should lead to the same minimizing film for the covering of Figure 6.

definition of $D(\mathcal{F})$. We can construct such a function by making it jump across a big sphere that encloses W with the sheet where its value is 1 that changes from 1 to 3. Then it is possible to take advantage of the fact that the wetting conditions are weak and with $u = 1$ on sheet 3 they do not impose wetting of e.g. $L_{1,1}$ resulting in the possibility (actually achievable) of an only partially wetted L_1 . Similarly for the other long edges. Clearly, however, such a surface cannot be a minimizer.

9. NUMERICAL SIMULATIONS AND CONCLUSIONS

A number of numerical simulations have been performed using the software code **surf** of Emanuele Paolini. It is based on a gradient flow with artificial viscosity starting from a triangulated surface having the required topology. It does not use the setting based on coverings of the present paper, however it gives a consistent result provided that: (i) the starting surface is the set $p(J_u)$ of some $u \in D(\mathcal{F})$; (ii) there is no change of topology; (iii) there is no touching of the invisible wires (they are not modelled by **surf**). Figures 7, 10 and 11 have all been obtained by starting from suitable faceted initial surfaces, with the geometry corresponding to the choice $h = 3.5$; for example the result shown in Figure 10 is obtained by starting from the faceted surface displayed in Figure 8.

Numerically it turns out that with $h = 3.5$ the area of the non-simply connected minimizer is slightly greater than the area of the conelike configuration; on the contrary increasing h to (e.g.) $h = 4$ results in a non-simply connected film surface that numerically beats the conelike configuration, consistently with the results of Section 6.

Decreasing h changes the minimizing evolution drastically: after a (large) number of gradient flow iterations, the film surface loses its symmetry (due to roundoff errors that break the symmetry of the problem) and one of the two tunnels shrinks at the expense of the other. The numerical evolution stops when the smaller hole completely closes, since the software cannot cope with changes of topology. Evolution after such singularization time depends on how the topology is modified. However it should be noted that the evolution would in this case typically impact with one of the invisible wires before the singularization time.

It is conceivable that for this value of h the evolution would produce a stationary surface, that is area-minimizing among surfaces that are forced to have the same symmetries of the boundary frame.

Decreasing h even further, in particular towards the value $h = \frac{\sqrt{2}}{2}$ that results in a regular tetrahedron, numerically produces an evolution where the two tunnels

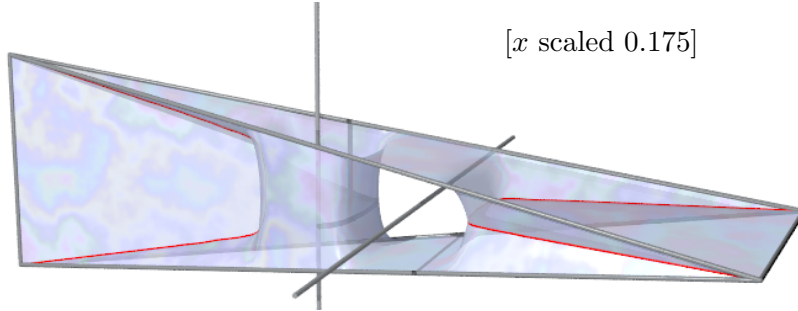


FIGURE 16. Minimal film obtained for $h = 20$. The resulting surface is scaled down in the x (right-left) direction of a factor of $3.5/20$ in order to match with the frame for $h = 3.5$ of Figure 8.

both shrink more or less selfsimilarly, so that we expect in the limit to obtain the area-minimizing cone of Figure 1 left.

On the other side we can explore what happens with ever increasing values of h (and a fixed sufficiently small value of s). Figure 16 shows the numerical solution for $h = 20$, where the x coordinate has been shrunk down in order to fit the same frame W of Figure 8. The resemblance of the result with the constructed surface Σ of Figure 8 is striking and suggest to conjecture that a minimizer $\Sigma_{\min} \in \mathcal{S}_{\min}(M_{h,s})$, when rescaled appropriately in the direction orthogonal to the short sides in order to have a fixed boundary, converges to Σ as $h \rightarrow +\infty$. This fact can be also motivated by observing that the area of a surface that is deformed by scaling of a factor k in the x direction can be computed by using an anisotropic version of the area functional $\int \phi(\nu) d\mathcal{H}^2$ with ϕ a positive one-homogeneous function having as unit ball the set $\{k^2x^2 + y^2 + z^2 \leq 1\}$, and ν a unit normal vector field. With increasing values of k the “vertical” portions of a surface (those with local constant x coordinate) pay less and less in anisotropic area and we expect that in the limit $k \rightarrow +\infty$ the anisotropic area to simply be given by the integral in x of the \mathcal{H}^1 measure of the sections of the rescaled surface with vertical planes parallel to the yz coordinate plane, so that a minimizer can be obtained by separately minimizing the size of each section. This would essentially lead to the faceted surface Σ of Figure 8.

REFERENCES

- [1] F.J. Almgren, *Existence and regularity almost everywhere of solutions to elliptic variational problems with constraints*, Mem. Amer. Math. Soc. **4** (1976), n. 165.
- [2] S. Amato, G. Bellettini, M. Paolini, *Constrained BV functions on covering spaces for minimal networks and Plateau’s type problems*, Adv. Calc. Var. **4** (2015), 1–23.
- [3] L. Ambrosio, N. Fusco, D. Pallara, *Functions of Bounded Variation and Free Discontinuity Problems*, Oxford Math. Monogr., Oxford, 2000.
- [4] K. Brakke, *Soap films and covering spaces*, J. Geom. Anal. **5** (1995), 445–514.
- [5] Y. Fang, *Existence of minimizers for the Reifenberg Plateau problem*, Ann. Sc. Norm. Sup. Cl. Sci. Pisa, **XVI** (2016), 817–844.
- [6] M. Giaquinta, G. Modica, J. Soucek, *Cartesian Currents in the Calculus of Variations I*, volume 37 *Ergebnisse der Mathematik und ihrer Grenzgebiete*, Springer-Verlag, Berlin Heidelberg 1998.
- [7] A. Hatcher, *Algebraic Topology*, Cambridge University Press, 2002.
- [8] R. Huff, *Conelike soap films spanning tetrahedra*, Trans. Amer. Math. Soc. **362** (2010), 5063–5081.
- [9] R. Huff, *An immersed soap film of genus one*, Comm. Anal. Geom. **19** (2011), 601–631.
- [10] G. Lawlor, F. Morgan, *Paired calibrations applied to soap films, immiscible fluids, and surfaces or networks minimizing other norms*, Pacific J. Math. **166** (1994), 55–83.

- [11] W. Magnus, A. Karrass, D. Solitar, *Combinatorial Group Theory: Presentations of Groups in Terms of Generators and Relations*, Dover Publications, 1976.
- [12] F. Morgan, *Geometric Measure Theory: A Beginners Guide*, Elsevier Science, 2008.
- [13] H.R. Parks, *Soap-film-like minimal surfaces spanning knots*, J. Geom. Anal. **2** (1992), 267–290.
- [14] E.R. Reifenberg, *Solution of the Plateau problem for m -dimensional surfaces of varying topological type*, Acta Mathematica **104** (1960), 1–92.
- [15] J. Taylor, *The structure of singularities in soap-bubble-like and soap-film-like minimal surfaces*, Ann. Math., **103** (1976), 489–539.